DEVELOPMENT OF A CANARD CONTROLLED ACTIVE STABILITY SYSTEM FOR A SOUNDING ROCKET

Theodore Youds, Benjamin Cradock, Liam Devlin, Jordan Whittaker, Joseph Daney de Marcillac

ABSTRACT

The Leeds University Rocketry Association (LURA) is aiming to beat the UK rocketry altitude record. This will be achieved in part using an active control system. This will help maintain a vertical attitude to use thrust more efficiently, leading to a greater apogee. Relevant literature is presented and reviewed. System requirements are outlined. System design is presented with brief reference to analysis conducted to this end. Manufacturing processes are considered. Challenges faced during assembly and testing are documented. Results from flight tests are analysed.

Keywords *— Sounding rocket, active control system, rocket stability.*

1. INTRODUCTION

The Leeds University Rocketry Association (LURA) was founded two years ago with the aim of 'Preparing the Mars Generation' (LURA, 2023). LURA aims to beat the UK amateur rocketry altitude record, currently at 36,274 ft (UKRA, 2021). This project builds on the work of Youds (2022) to develop an active control system that improves the dynamic stability of future LURA rockets, allowing them to fly straighter, and therefore higher. Canard actuated control was selected over other methods such as thrust vectoring due to space constraints around the solid rocket motor. The control system was named Aptos.

After concluding that this system was unable to be integrated with existing LURA rockets, a new rocket testbed was required, named Pathfinder. This was developed by the project group with the purpose of testing Aptos and future LURA active control systems and so was designed to be durable - the body tubes and the nose cone were off-the-shelf components made of fibreglass. The rocket operated a simple recovery system, where a small charge would pressurise the recovery chamber and split the rocket in two during descent, releasing the parachute. The risers were connected to eyebolts on both the upper and lower parts of the rocket. The rocket features a Delrin spin-can at the base, mounted on bearings, enabling the rear passive fins to rotate about the rocket's longitudinal axis to mitigate the effects of canard downwash. Delrin is a hard plastic with a high yield strength and relatively low density, that is easy to machine and can be tapped (Protolabs, 2020).

System design required aerodynamic analysis of the canards, mechanical design of the module, actuator selection and electronics design, control algorithm creation and integration of these sub-systems. This would be followed by manufacture, assembly and test, including a further stretch objective to perform a flight test which would verify the system's performance and stability. Aspects of these objectives will be discussed in this report as well as the results from the flight tests performed.

The project followed a design process simplified from the NASA Systems Engineering Handbook (Hirshon et al., 1995). A preliminary design review (PDR) and a critical design review (CDR) were conducted to allow academic staff and the project's industrial sponsors, Collins Aerospace, to review the design and provide technical advice. Prior to the flight test campaign, a mission readiness review (MRR) was conducted. The purpose of these reviews was to catch design problems early in the process and ensure smooth system integration down the line.

2. LITERATURE REVIEW

This literature review will first detail the background theory to rocket stability and active control before exploring existing research relevant to the project.

2.1. Rocket Stability and Active Control

Stability refers to the ability of a vehicle to restore itself after a disturbance, which for a rocket could be a wind gust. A rocket is classed as stable when the centre of pressure (CP) is more than one body diameter behind the centre of gravity (CG) because this means the lift force from the rear fins provides a restoring moment (NAROM Andøya Space Centre, 2018) . The reference to body diameter is a normalised measure called 'stability margin' and this should be greater than one (Guerrero et al., 2018). The main issue with passive rocket stability is that the rocket body 'weathercocks' in the presence of a crosswind. The lift force from the rear fins rotates the rocket and hence rotates the rocket body into the wind (Bellis, 2019). This creates a horizontal component of thrust which reduces the apogee of the rocket (Buchanan et al., 2015).

Active control is a solution to weathercocking, aiding in maintaining a vertical attitude and use thrust

more efficiently. Active control can be achieved either aerodynamically or through Thrust Vector Control (TVC), where the engine nozzle is gimballed to change the direction of thrust (Schinstock et al., 2001). The advantage of TVC is that it is independent of rocket velocity and so is effective at low velocities unlike aerodynamic control (Asselin, 2021). However, it is very complex to implement with off-the-shelf solid rocket motors and so comes with significantly increased cost.

In contrast, aerodynamic control deflects fins to alter the airflow and generate a moment to steer the rocket. This can be done with the existing rear fins or additional fins near the rocket's nose called canards. Canards induce more drag (Montalvo and Costello, 2011) but can generate more torque due to their distance from the CG increasing their sensitivity (Gutman, 2003). Rear fins also come with the added complexity of reduced space to position actuators around the rocket motor.

2.2. Existing Relevant Research

There is extensive literature available on the aerodynamic analysis of canards, including computational fluid dynamics (CFD) simulations (Chen et al., 2017), as well as the modelling and simulation of an active control system (Jang et al., 2011; MacLean, 2017). There are also plenty of student (DARE, n.d.) and hobbyist (Anon, 2021) examples of practical developments and implementations of active control systems.

A team from Worcester Polytechnic (Alvarez et al., 2019) performed mechanical, electronic and control design on a system that actuated tabs on passive rear fins (like an elevator tab on an aircraft's horizontal stabilizer). They also manufactured and tested the system and although benchtop testing was successful, the rocket did not leave the launch pad so they couldn't demonstrate the system functionality. They highlighted difficulties positioning the actuators near the rocket motor and ended up fixing them outside the rocket body which adds unnecessary drag.

A team from Santa Clara (Guerrero et al., 2018) performed modelling of a canard-controlled rocket. They performed control and electronics design but not mechanical design and only prototyped the system before the project deadline. However, they did identify the next step as focusing on the drivetrain.

The report written by the University of Canterbury team (Buchanan et al., 2015) describes the development of a rocket that set the altitude record for an I-class motor. As a report on the entire rocket, the control system is only briefly touched upon although the mechanical design is well-detailed. The report also includes the successful flight tests and highlights that the actuation system 'performed very well'.

A team from TU Delft (DARE, n.d.) produced a canard-controlled rocket, although no technical documentation could be found. They could only implement control in the roll axis but concluded that weathercocking was reduced, and apogee was increased. However, they highlighted that the canards produced a downwash that affected the passive fins. These findings led to the implementation of a spin-can on Pathfinder.

An analysis of this literature would conclude that the nature of the project is challenging, with only one university team (University of Canterbury) successfully implementing an active control system for three axis control. There is a great need for attention to detail when designing the control system as well as for the testbed – the Pathfinder rocket by itself must function properly so that the control system can be tested. This review also highlights that rear fin control brings difficulties due to space restrictions around the motor tube and that canard downwash must be considered for canard-control.

3. CONCEPT OF OPERATIONS AND REQUIREMENTS

Before design started on the Aptos module, a concept of operations (CONOPS) was established in order to derive the system requirements. The CONOPS shown in Fig. 1 shows the key stages of the system, agnostic to any specific design solutions. The process was linear, except for the possibility of failure instead of apogee detection. As progress in the design stage was made, the requirements (contained in full in Appendix A) and CONOPS evolved continuously due to new discoveries and issues that were encountered. However, the top-level requirements hardly changed. These are shown in Table 1. One top-level requirement was introduced during development: the ability to interact with the module whilst it was assembled in the rocket (APT-REQ-7). Failure to satisfy this requirement would have led to difficulty during launch procedures, potentially rendering the module ineffective.

Design decisions were always based on meeting the requirements. This allowed for continuous monitoring of whether requirements were being met, improving early error detection. These requirements were reviewed at key decision points throughout the project, including the PDR and CDR. The effectiveness of the design was always evaluated in the context of whether it met the requirements.

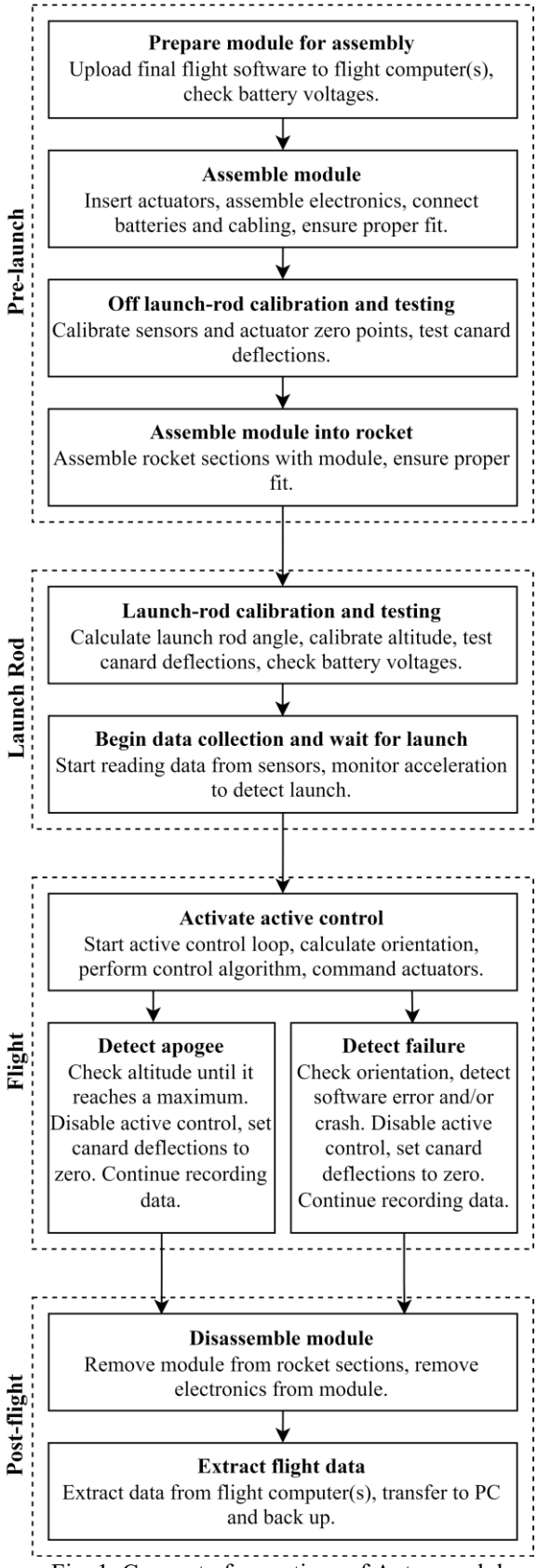

Fig. 1. Concept of operations of Aptos module.

Table 1 – Top-level Aptos system requirements

ID	Requirement
APT-REQ-1	The system shall improve the rocket's ability to maintain a vertical flight by minimising roll rate and pitch and yaw Euler angles during ascent.
APT-REQ-2	The system shall maintain structural integrity during flight.
APT-REQ-3	The system shall integrate with a rocket of 4" body diameter.
APT-REQ-4	The system shall fail safely.
APT-REQ-5	The system shall be manufacturable in-house within time and budget constraints.
APT-REQ-6	The rocket should fly higher with the Aptos module installed than without it.
APT-REQ-7	The system shall be able to be controlled without disassembling the rocket.

4. SYSTEM DESIGN AND MANUFACTURE

4.1. Module Design Overview

The Aptos system was designed to be a self-contained module which integrated directly into Pathfinder with couplers at both ends, forming part of the rocket body. This meant the control module was easily accessible which improved the test, inspection and data extraction procedures. This configuration also had a secondary benefit: the module weight was supported axially through the rocket body load path as opposed to through radial screws which would be loaded in shear. The module was designed in SOLIDWORKS, a 3D mechanical CAD package. Fig. 2 is an exploded view of the system assembly.

The module consisted of a Delrin casing (Detail 1), with an upper recess to house the servos and a lower pocket to contain the Printed Circuit Boards (PCBs). The canards were then mounted to the servos through drilled holes.

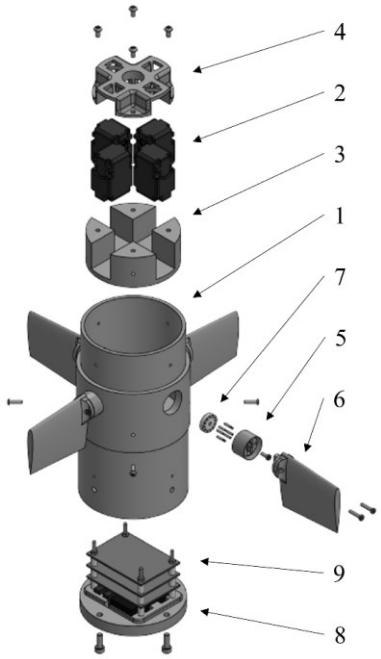

Fig. 2. Exploded View Of Module Assembly

The module casing was machined from solid Delrin, consistent with the Pathfinder Spin Can. The casing was designed with manufacturing processes in mind and so was easy to produce, starting with lathe operations to turn the couplers and bore the servo recess, before milling the lower pocket, drilling the necessary holes and tapping as required.

The servos (2) were positioned by a 3D printed seat (3) which was fixed to the module by radial screws and then secured in place with a 3D printed bracket (4). This sub-assembly considered design-for-assembly (DFA) principles and so incorporated rotational symmetry as well as stacking components in a single axis (Boothroyd, 1994).

Servo dimensions allowed for direct drive of the canards. This was implemented for mechanical simplicity. The drivetrain design required an intermediate part ('interface') (5) between the canard (6) and the servo horn (7) as it was impractical to insert the central servo screw through the whole span of the canard. The interface used dowel pins to transfer torque from the servo (horn) and used the servo screw to provide axial fixing. A chamfer-and-key fit, with its inherent high friction, prevented torque loss between the interface and the canard. The complex geometry of the canard meant 3D printing was the appropriate manufacturing technique.

A 3D-printed base (8) incorporated a custom profile to secure the batteries that powered the PCB stack (9) and the servos. The milled pocket had channels down the sides of the PCB stack to allow space for wiring and a central conduit allowed wiring to pass from the lower pocket to the upper atrium.

4.2. Canards

The canards were designed such that they could produce enough torque to steer the rocket. As a starting point, an appropriate canard cross-section was determined. To do this, XFOIL was used. XFOIL is a low fidelity CFD software which implements panel methods and was useful for this project as it allows relatively quick comparison of aerofoil shapes compared to CFD (Drela, 1989). The software is limited in accuracy but for initial cross section design, its speed outweighed its flaws.

Using this software, multiple aerofoil shapes, along with flat plates, were compared. Flat plates were desirable due to their drag characteristics, but their lift characteristics were inferior to standard NACA aerofoils (Daney de Marcillac, 2023). They were also more difficult to model due to the limitations of XFOIL. A high lift-to-drag (L/D) ratio was used as the driving selection parameter. The drag force needed to be sufficiently low so that it could be neglected within the control algorithm, simplifying linearisation (Youds, 2023). Using this method, the NACA 0014 aerofoil was selected (Whittaker, 2023).

The canards needed to produce enough torque overcome the corrective moment of the rocket, which is produced by the lift from the passive fins and the rocket body. This moment, obtained through OpenRocket (Daney de Marcillac, 2023) was equated to the torque generated by the canards to produce a minimum surface area and lift coefficient (C_L) requirement. As suggested by Guy et al. (1999), a low aspect ratio, low taper and unswept wing shape was chosen. The dimensions were varied and inputted into XFLR5 to obtain their maximum lift coefficient. This is a software based on XFOIL that allows 3D wing aerodynamic analysis. This process was repeated until a minimum surface area was obtained that matched the lift requirements. The canards had a root and tip chord of 60 mm and 50 mm respectively and a span of 70 mm. The corresponding $C_{L\alpha}$ (coefficient of lift with respect to angle of attack) curve was then implemented into the control algorithm. A wind tunnel test was performed to validate the data from XFLR5, however the data was inconclusive due to faulty load cells in the wind tunnel (Whittaker, 2023).

The canards were 3D printed out of ABS filament as it is stronger than the more commonly used PLA filament (Engineers Edge, 2023). The ability to 3D print them reduced the lead time for manufacture allowing for rapid prototyping. An infill of 40% was used to ensure adequate strength.

4.3. Actuators

It was decided that off the shelf actuators would be used to control the canards as they are widely available. Smart servo motors were chosen over stepper motors as they maintained high torque throughout actuation and had position feedback with a PID feedback loop built in and the use of a potentiometer (Youds, 2023). The canards would experience a certain pitching moment during flight and the servos were chosen to have enough torque to overcome this. Equation 4.1 was used to calculate the pitching moment (Clancy, 1983).

$$M = C_m \bar{q} S \bar{c} \tag{4.1}$$

Where C_m is the pitching moment coefficient, obtained from XFLR5 (Appendix B), $\bar{q}$ is the dynamic pressure, S is the wing area and $\bar{c}$ is the average chord length. This yielded a required torque of 7.95 kg.cm so an 11 kg.cm servo was chosen (safety factor of 1.4).

4.4. Electronics

The electronics subsystem provided the means of acquiring data, running control software, and commanding the actuators. Design of the system architecture and component selection were primarily influenced by the need to fit the mechanical size constraints and mitigation of any potential failures.

Due to the large number of tasks to be run by the flight computer, it was necessary to introduce a second microcontroller to provide redundancy on the most important failsafe: detecting whether the orientation of the rocket was out of limits. This provided a hardware failsafe, reducing the reliance on software to ensure a safe system.

Another set of failures pertained to powering the microcontrollers (primary and monitor) and actuators. The system architecture (shown in Appendix C) was designed such that the batteries were separate so that one power failure would only affect one controller at a time. Additionally, the voltage of the actuator battery, which had the highest current draw, could be read minutes before flight to ensure there was enough energy for canard deflection.

Once the system architecture was complete and reviewed, detailed design was performed using KiCAD, a free electronic computer aided design software (KiCAD Development Team, 2023). All the selected components were entered into electronics schematics, including smaller components such as resistors and capacitors and connections between components.

Following this, the components were physically laid out in the PCB editor. It quickly became apparent that to fit the mechanical size constraints, three PCBs were required, requiring some iteration between the schematics and PCBs. Both the final schematics and PCB designs are shown in Appendix D.

Assembly and manufacture consisted of soldering off-the-shelf components onto the PCBs, as well as some mechanical integration onto the structural components of the module. Each component was tested prior to assembly as well as after, including continuity testing and individual component tests using breadboards. This testing process highlighted a faulty Bluetooth module. Switching this component was a significant task due to having to desolder and resolder the new component.

4.5. Control Algorithm

4.5.1. Closed Loop Control

The Aptos system used a linear quadratic regulator (LQR) to maintain vertical flight during ascent. Onboard sensors measure the rocket's attitude and attitude rates and subsequently estimate the rocket's state, $\mathbf{x} \in \mathbb{R}^6$, given by

$$\mathbf{x} = \{\phi \quad \theta \quad \psi \quad p \quad q \quad r\}^T, \tag{4.2}$$

where ϕ, θ and ψ are the roll, pitch and yaw angles, and p, q, and r are their rates.

The controller aimed to minimise this state vector by controlling the four canard deflections that comprise the input vector, $\mathbf{u} \in \mathbb{R}^4$, defined as

$$\mathbf{u} = \{x_1 \quad x_2 \quad y_1 \quad y_2\}^T, \tag{4.3}$$

where x_1 and x_2 are the canard deflections that control the pitch axis, and y_1 and y_2 control the yaw axis.

Crosswinds during flight can induce an angle of attack, α, or sideslip angle, β, on the rocket, and these generate unwanted pitch and yaw moments that draw the rocket off its vertical trajectory. These angles were not known by the controller, and therefore were modelled as disturbances. The disturbance vector, $\mathbf{d} \in \mathbb{R}^2$ is given by

$$\mathbf{d} = \{\alpha \quad \beta\}^T. \tag{4.4}$$

4.5.2. Dynamic Modelling

To tune the LQR controller, a linear model of the system dynamics was required in the form of a state space equation. First, equations were derived for each of the moments that act on the rocket during flight. Detail is included in the work of Youds (2023), but a brief summary is included here.

It was assumed that there were three moments acting in the rocket's pitch and yaw axes. Here, M denotes a pitching moment, N denotes a yawing moment, and L a rolling moment.

When flying at an angle of attack (or sideslip angle), the lift generated by the rear fins generates a torque that turns the rocket towards the incoming air (Mandell et al., 1973). These are the corrective moments, M_{corr} and N_{corr}.

As the rocket rotates, aerodynamic drag induces moments, L_{damp}, M_{damp} and N_{damp}, that counteract its motion. These are proportional to the rocket's attitude rates in the respective axis (Mandell et al., 1973).

Finally, lift forces generated by the canards induce torques in all three axes, L_{can}, M_{can} and N_{can}, that help to steer the rocket. Drag was neglected in the derivation of the canard moments due to the high L/D ratio of the aerofoil (Daney de Marcillac, 2023). Therefore, they are only dependent on the canard deflections and the angle of attack and sideslip angle.

The resultant moment vector on the rocket was then derived to be

$$\mathbf{M} = \begin{Bmatrix} L_{can} - L_{damp} \\ M_{can} - M_{corr} - M_{damp} \\ N_{can} - N_{corr} - N_{damp} \end{Bmatrix}. \quad (4.5)$$

Euler's Rotational Equation of Motion was used to relate this to the rocket's attitude rates, $\boldsymbol{\omega}$, and accelerations, $\dot{\boldsymbol{\omega}}$, by its moments of inertia, J, as shown in (4.6).

$$\mathrm{J}\dot{\boldsymbol{\omega}} + \boldsymbol{\omega} \times (\mathrm{J}\boldsymbol{\omega}) = \mathbf{M} \quad (4.6)$$

This model was linearised using a first order Taylor series and small angle approximations to form a state space equation of the form,

$$\begin{aligned} \dot{\mathbf{x}} &= \mathrm{A}\mathbf{x} + \mathrm{B}\mathbf{u}, \\ \mathbf{y} &= \mathrm{I}_6\mathbf{x}, \end{aligned} \quad (4.7)$$

where A and B are the state and input matrices, and I_n is the $n \times n$ identity matrix.

4.5.3. Control System Tuning

Tuning the LQR controller was achieved by varying the state-cost weighted matrix, Q, and the input-cost weighted matrix, R. The MATLAB function `lqr(A, B, Q, R)` was then used to calculate the optimal gain-set.

Minimising the pitch and yaw angles was made a higher priority than their rates, as this smoothed the canard motion significantly, thus reducing the chance of dynamic stall and other more complex aerodynamic effects.

In the roll axis, the rate was much more important than the angle. If the rocket starts to roll, the controller should stop it but not try to return to its original roll angle, as this will come at the cost of pitch and yaw controllability. Therefore, the roll angle weighting was reduced to near zero, and the roll rate was weighted equally to the pitch and yaw angles.

All four actuators were identical and therefore the R matrix was used to penalise the use of all actuators equally. For the initial active control flight tests, the actuators will be heavily penalised, but this will likely be reduced in the future once the system's performance has been verified.

4.5.4. System Performance and Robustness

A nonlinear model of the system dynamics was created in the modelling software Simulink and was used to test the control system's performance.

Fig. 3 shows how the system responded to a constant 5 m/s crosswind acting only in the pitch axis. This is compared with the free response without the canard control system.

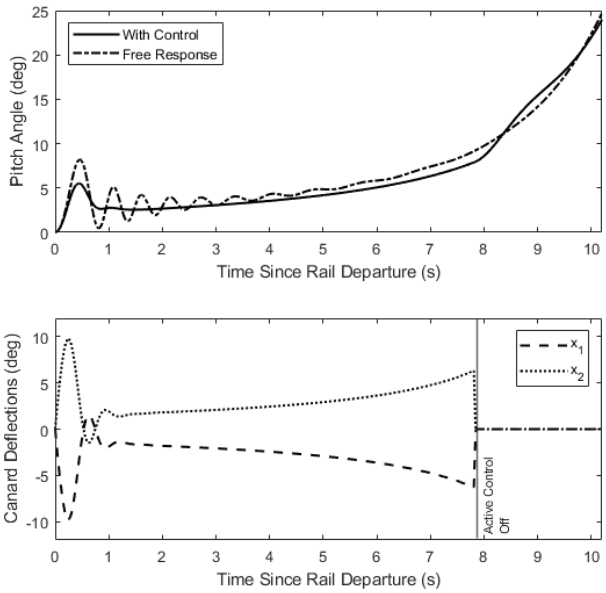

Fig. 3. Performance of the Aptos system compared to the Pathfinder's free response in the presence of a 5 m/s constant crosswind.

Since there were no roll moments, the x_1 and x_2 canards acted symmetrically to reduce the pitch perturbations generated by the wind. The initial off-rail pitch angle was reduced by 2.7° and the following oscillations were damped almost immediately.

Significant performance improvements could be made by reducing the R matrix and allowing the canards to deflect beyond 10°.

4.6. Software

The main task of the software was to implement the control algorithm, including determining the state from sensors and communicating over the correct protocol with the actuators (Cradock, 2023). Managing failures was also important.

An additional consideration was the usability of the system whilst assembled with the rocket. This was necessary to check that the system was still operational before flight, as well as perform calibration on the launch rail.

A state machine architecture was selected, allowing the software to change between modes depending on user interaction or detection of failures. This also made debugging and testing significantly easier as the current state could easily be recorded, narrowing down the search for errors.

All the software was written in C++, separated into modules to improve readability and provide enough abstraction such that the primary and monitor controllers could share large amounts of code.

4.7. Integration Considerations

Embedded software development for microcontrollers is more involved than for application software as testing requires access to the electronics hardware. This meant that integration and testing of the software and electronics was only possible once both were close to completion.

For example, the coordinate system of the sensors was determined by their placement on the PCBs, which was different to the coordinate system used by the control algorithm. Therefore, a coordinate system transformation was required at some point in the software, dependent on the electronics design. This was overcome by simply applying the transformation before any calculations (Cradock, 2023). A simple test was performed to ensure the measured values were in the control system coordinates, not the physical coordinate system of the sensors.

A key feature of the flight computer was the ability to interact with it wirelessly over Bluetooth (both microcontrollers separately). Integration of this feature between software and hardware was vital as it was necessary for faster integration and testing of other features. Due to different hardware between the primary and monitor controllers, the software for Bluetooth communication also had to be different – fortunately, due to the modular design of the software, this change did not significantly impact the difference between the two code packages. (Cradock, 2023)

The mechanical manufacture and assembly of the module proved challenging in various ways. The dowel diameter (3) had to be estimated in the design phase as there was no information available relating to the diameter of the servo horn holes. Unsurprisingly therefore the holes had to be widened during assembly. This highlighted a common issue faced in systems engineering whereby interfacing off the shelf components with in-house components can be problematic.

Another issue encountered involved the dowel holes in the interface. These holes required a tight tolerance to effectively transfer the torque from the servo to the canards. Due to differing print conditions and filaments used in the prototyping phase, the prints differed slightly in dimensions. The dowel holes were adjusted several times however the inconsistent prints made it difficult to pick the correct diameter. Using the same equipment throughout the prototyping phase would have negated this issue.

A flaw in the overall design process was submitting mechanical parts for manufacture before electronic design was finished. Ideally, both would be completed concurrently and if data has been transferred across domains accurately, this should avoid any complications during integration (Alvarez Cabrera et al., 2010). However, this was impossible due to the lead times on the mechanical parts.

The result of this was that the lower pocket milled out for the PCB stack was not deep enough and the cables wiring up through the conduit to the servos would have been excessively bent and susceptible to damage. The solution was to merge the battery board and the PCB stack base plate as the base plate which dropped the height of the entire stack and created clearance between the top PCB and the top of the pocket.

5. FLIGHT TEST DISCUSSION

The launch weekend planned for three flights, with one acting as a control test to demonstrate the effectiveness of Pathfinder by commanding the canards to maintain zero deflection and the remaining two to demonstrate active control. Unfortunately, the servo motors were damaged during the recovery of the first flight, and it was deemed unsafe to try and launch with active control. However, a second launch was still conducted to collect more data which can be used to further improve the software.

5.1. Data Acquisition

The primary focus of both test flights was collecting enough data to increase confidence in the software and control algorithm. As planned, data from both the primary and monitor controller SD cards was

extracted immediately after recovery and subsequently decoded. Unfortunately, after the first flight, it became apparent that a software bug prevented the barometer data from being saved onto the SD cards, and therefore the altitude and vertical velocity profiles were not captured. This was fixed for the second flight, and all analysis on the first flight data used the same altitude and velocity profiles as the second flight.

Also obtained during the flight was the target canard deflections which could be used to determine whether the control system was performing as expected. Due to also collecting all the sensor data, the control gains could be tweaked and rerun on the exact same orientation. Additionally, both controllers recorded the time delay between each iteration of code. This indicated that optimization would be required for the primary controller to improve control performance (Cradock, 2023).

Overall, the data acquisition was a success despite not recording barometer data on the first flight. The quantity of data collected could significantly improve the confidence in the control system through further analysis and reruns if required.

5.2. Altitude Discrepancy

As mentioned in Section 5.1, altitude was only recorded on flight 2. This data is presented in Fig. 4 along with the predicted altitude from the OpenRocket model.

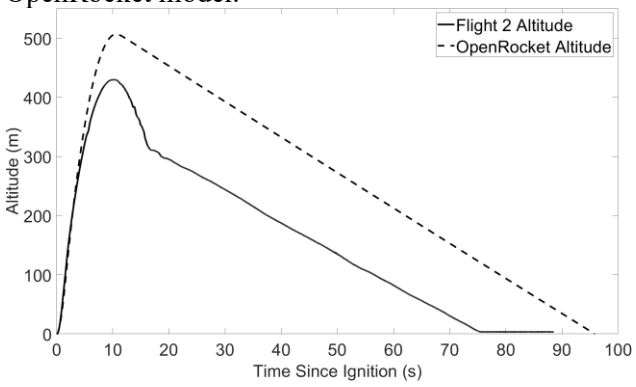

Fig. 4. Flight vs OpenRocket Altitude

The apogee, as recorded by the flight computer, was 429.76 m while the predicted altitude from OpenRocket was 506.71 m, equating to an error of 17.9% which exceeds the OpenRocket software validation report of 10-15% (Niskanen, 2013; Calcara et al., 2016). However, the time of apogee was very accurate with an error of only 3% which suggests the rocket's velocity was lower than expected. This was likely down to discrepancies between the drag model used in OpenRocket and the actual drag. The software was not able to simulate imperfections on the rocket body, meaning the skin drag was greater than predicted. There were also small gaps along the rocket body, such as between the canards and the module wall, which would add interference drag that OpenRocket could not account for. Finally, the spin-can on the Pathfinder rocket could have increased the drag. The spin-can had a lower moment of inertia than the whole rocket meaning it could spin up faster, extracting kinetic energy from the rocket and doing work on the surrounding air. Kinetic energy could also have been lost through friction losses in the bearings. Another launch with the spin-can fixed to the rocket would be necessary to confirm this (Daney de Marcillac, 2023).

5.3. Rocket Performance

Fig. 5 presents the roll, pitch and yaw angle data collected during the ascent of the second flight. As soon as the rocket leaves the rail, it begins to roll, likely due to a slight misalignment of the canards.

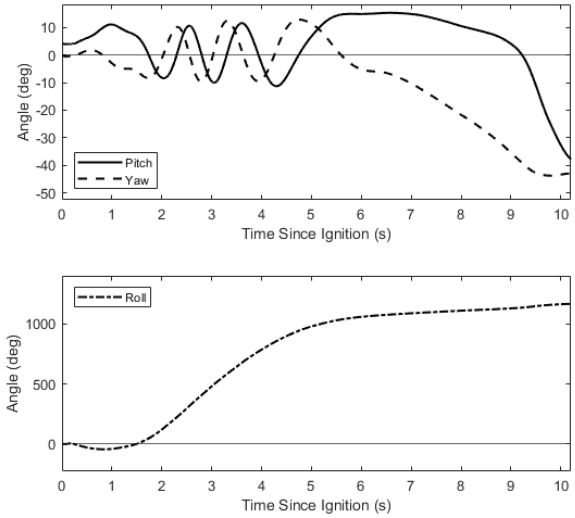

Fig. 5 Roll, pitch, and yaw angle data collected during flight 2 ascent

Approximately one second later, the direction of the roll reverses. This was not seen in any previous LURA flights and the exact cause is not currently known. It is likely that the spin-can started to spin in the opposite direction to the rocket body, and frictional forces in the bearings resisted the rocket's existing roll motion, eventually reversing it entirely.

Throughout the ascent, the rocket only rolled through approximately 3 ¼ revolutions. It was expected that a rocket with such a low radial moment of inertia would roll significantly more, and therefore this indicates that the spin-can likely helped to mitigate this. There were no sensors on the spin can,

so its performance cannot be fully verified. However, this data indicates that it likely worked as expected.

The pitch and yaw motion seen in Fig. 5 is perfectly characteristic of a passively stable, spinning rocket. Perturbations due to the wind cause the rocket to precess in a motion known as 'coning', identified by the out of phase sinusoidal waveforms (Youds, 2022).

5.4. Control System Performance

Throughout the flight, the primary controller commanded the servos to hold zero deflection. However, the desired deflections were still calculated to examine the simulated performance of the control system to real input data, and these are displayed in Fig. 5. As soon as the active control was enabled, the canards all deflected in the same direction to counteract the roll motion shown in Fig. 5. As the roll direction reversed, so did the canard deflections. The LQR controller was tuned to minimise the roll rate, as opposed to the roll angle and the data indicates that this performed well. The canards reacted to the high roll rate in the first few seconds of flight but started to return to zero as a steady state roll rate was reached following motor burnout. The magnitude of the deflections reached a maximum of about 80°, as they had no effect on the motion of the rocket since the servomotors were not actually deflecting.

In future flight tests, when the system is in control of the rocket, the canard deflections will be limited to $\pm 10°$, and the primary controller will prevent them from actuating at all when the rocket is rolling at high rates. Whilst trying to minimise the rocket's roll rate, the canards also acted in pairs to reduce the coning motion seen in Fig. 5. Again, the magnitude of the deflections calculated here were significantly higher than what is expected when Aptos has control, but the pattern is correct.

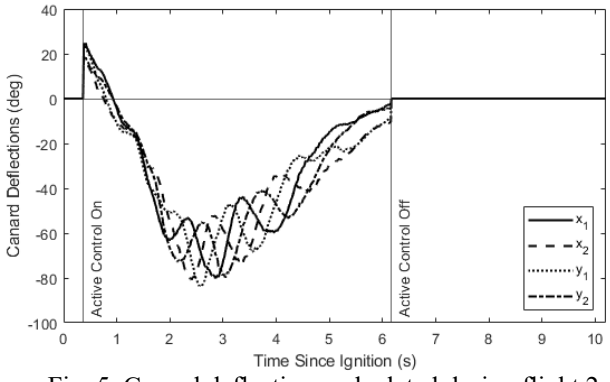

Fig. 5. Canard deflections calculated during flight 2.

Overall, the predicted canard deflections indicate that the system behaved as expected. Nothing alarming has been identified in the flight test datasets and therefore in future flights, the controller will be activated and will command the servomotor deflections to steer the rocket.

6. CONCLUSION AND FUTURE WORK

Despite not being able to validate the performance of the control system, Project Aptos successfully delivered on its aim to develop an active control system. The following objectives, as laid out in the projects CPP were all achieved (Daney de Marcillac et al., 2022).

Canard aerofoil and planform design was successfully undertaken, and aerodynamic analysis was performed. A shortcoming of the project was the lack of aerodynamic data validation due to faulty load cells in the university wind tunnel. Mathematical and Simulink models were created which performed dynamic analysis after which a functioning control algorithm was successfully developed. Appropriate hardware was selected using the requirements laid out. A linkage system was designed and implemented which, after integration with electronics within the module, was proven to work. Parts were ordered and manufactured successfully to allow a full assembly of the module and rocket before the allocated launch weekend. Test plans and procedures were written effectively and proved useful in reducing error during assembly. All benchtop testing either confirmed the functionality of a component or helped to troubleshoot issues.

Adding to these achievements, two flight tests were performed, collecting valuable data about the flight dynamics of the rocket with canards set to zero degrees. Unfortunately, no flight was performed with the active control system switched on, but this was due to damage sustained by a servo upon recovery rather than the control algorithm. Despite this, these initial flights will pave the way for future launches with the canards providing active control.

Future work includes, but is not limited to, validating the aerodynamic data by performing wind tunnel tests with an accurate set up, performing a design optimisation analysis on canard aerofoil and planform design and including drag in the control algorithm. More servo testing must also be done to assure higher quality servos are purchased in future flights to reduce the probability of failure. The PCB stack design should be reconsidered in light of issues with assembly encountered before launch. Further investigation into the spin-can should also be done to see the effects on expected altitude of apogee.

Overall, Project Aptos has been a huge success. It was an important next step for LURA and

allows future teams to continue the work performed by group members. This system marked the first step in enabling future flights to compete for the UK Student Altitude record.

REFERENCES

Alvarez, A., Gerhardt, G., Kelly, E., O'Neill, J. and Whitehouse, J. 2019. *Design and Integration of a High-Powered Model Rocket-II*. BSc Aerospace Engineering, Massachusettes: Worcester Polytechnic Institute.

Alvarez Cabrera, A.A., Foeken, M.J., Tekin, O.A., Woestenenk, K., Erden, M.S., De Schutter, B., van Tooren, M.J.L., Babuška, R., van Houten, F.J.A.M. and Tomiyama, T. 2010. Towards automation of control software: A review of challenges in mechatronic design. *Mechatronics*. **20**(8), pp.876–886.

Anon 2021. *Fineas - Active Fin-Controlled Model Rocket* [Online]. BPS Space. Available from: https://www.youtube.com/watch?v=iuuH9-pyKHI.

Asselin, M. 2021. *Operational aircraft performance and flight test practices* 1st ed. Reston, Virginia: American Institute of Aeronautics and Astronautics, Inc.

Bellis, M. 2019. The History of Flight Control Systems. *ThoughtCo*. [Online]. [Accessed 2 May 2023]. Available from: https://www.thoughtco.com/rocket-stability-and-flight-control-systems-4070617.

Boothroyd, G. 1994. Product design for manufacture and assembly. *Computer-Aided Design*. **26**(7), pp.505–520.

Buchanan, G., Wright, D., Hann, C., Bryson, H., Snowdon, M., Rao, A., Slee, A., Sültrop, H., Jochle-Rings, B., Barker, Z., McKinstry, A., Meffan, C., Xian, G., Mitchell, R. and Chen, X. 2015. The Development of Rocketry Capability in New Zealand—World Record Rocket and First of Its Kind Rocketry Course. *Aerospace*. **2**(1), pp.91–117.

Calcara, L., Fernandez, monica, Green, C. and Hosokawa, T. 2016. *High Power Rocket Design Report*. Los Angeles: Loyola Marymount University.

Chen, Y.-C., Gao, X.-B., Gao, M. and Lv, H.-M. 2017. Aerodynamic characteristic of a canard guided rocket. *International Journal of Modeling, Simulation, and Scientific Computing*. **08**(01), p.1750001.

Clancy, L.J. 1983. *Aerodynamics* Repr. London: Pitman.

Cradock, B. 2023. *Design and Development of an Embedded Flight Computer for a Canard-Controlled Sounding Rocket*. Masters Thesis, Leeds: University of Leeds.

Daney de Marcillac, J. 2023. *Design and Aerodynamic Analysis of a Canard-Controlled Sounding Rocket*. Leeds, UK: University of Leeds.

Daney de Marcillac, J., Youds, T., Devlin, L., Whittaker, J. and Craddock, B. 2022. Project Aptos Contract Performance Plan.

DARE n.d. Advance Control Team. *DARE*. [Online]. [Accessed 20 April 2023]. Available from: https://dare.tudelft.nl/projects/act/.

Drela, M. 1989. XFOIL: An Analysis and Design System for Low Reynolds Number Airfoils *In*: T. J. Mueller, ed. *Low Reynolds Number Aerodynamics*

Engineers Edge 2023. ABS Plastic Filament Engineering Information. *Engineers Edge*. [Online]. [Accessed 1 May 2023]. Available from: https://www.engineersedge.com/3D_Printing/abs_plastic_filament_engineering_information_14211.htm.

Guerrero, V., Barranco, A. and Conde, D. 2018. Active Control Stabilization of High Power Rocket. *Mechanical Engineering Senior Theses*.

Gutman, S. 2003. Superiority of Canards in homing missiles. *IEEE Transactions on Aerospace and Electronic Systems*. **39**(3), pp.740–746.

Guy, Y., Morrow, J. and McLaughlin, T. 1999. The effects of canard shape on the aerodynamic characteristics of a generic missile configuration *In*: *24th Atmospheric Flight Mechanics Conference*. Portland,OR,U.S.A.: American Institute of Aeronautics and Astronautics.

Hirshon, S., Voss, L. and Bromley, L. 1995. *NASA Systems Engineering Handbook*. Washington D.C.: NASA.

Jang, J.-W., Alaniz, A., Hall, R., Bedrossian, N., Hall, C. and Jackson, M. 2011. *Design of Launch Vehicle Flight Control Systems Using Ascent Vehicle Stability Analysis Tool* . Houston, TX: The Charles Stark Draper Laboratory.

KiCAD Development Team 2023. KiCAD. Available from: https://www.kicad.org/.

LURA 2023. Our Mission. *LURA*. [Online]. Available from: https://leedsrocketry.co.uk/mission/.

MacLean, S.M. 2017. *Modeling and Simulation of a Sounding Rocket Active Stabilization System*.San Luis Obispo, California: California Polytechnic State University.

Mandell, G.K., Caporaso, G.J. and Bengen, W.P. 1973. *Topics in advanced model rocketry*. Cambridge, Mass: MIT Press.

Manimaran, H.P., Khaja Naib Rasool Shaik, Gopi Kompelli, and Kaunas university of technology 2020. Stability Analysis of Conventional Rocket Model using CFD Tool. *International Journal of Engineering Research and*. **V9**(01), IJERTV9IS010262.

Montalvo, C. and Costello, M. 2011. Effect of canard stall on projectile roll and pitch damping. *Proceedings of the Institution of Mechanical Engineers, Part G: Journal of Aerospace Engineering*. **225**(9), pp.1003–1011.

NAROM Andøya Space Centre 2018. Aerodynamics and forces acting on the rocket. *NAROM Student Rocket Pre-Study*.

Niskanen, S. 2013. OpenRocket technical documentation. [Accessed 3 January 2023]. Available from: https://openrocket.info/documentation.html.

Protolabs 2020. *Protolabs*. [Online]. [Accessed 2 May 2023]. Available from: protolabs.com.

Schinstock, D.E., Scott, D.A. and Haskew, T.A. 2001. Transient Force Reduction in Electromechanical Actuators for Thrust-Vector Control. *Journal of Propulsion and Power*. **17**(1), pp.65–72.

UKRA 2021. UK Rocketry Altitude Records | UKRA - United Kingdom Rocketry Association. [Accessed 3 November 2022]. Available from: http://ukra.org.uk/records/allclass.

Whittaker, J. 2023. *Level 4 Individual Project Report*. Masters Thesis, Leeds: University of Leeds.

Wyatt, D. 2007. *An Actively Stabilised Model Rocket*.[Online] Fourth-year Undergraduate. Available from: http://aeroconsystems.com/tips/Active_Stabilized_rocket_Wyatt.pdf.

Youds, T. 2023. *Development Of An Active Control System For A Canard-Controlled Sounding Rocket*. Masters Thesis, Leeds: University of Leeds.

Youds, T. 2022. Feasibility Analysis of a Reaction Wheel System for Sounding Rocket Roll Control.

APPENDICES

This page intentionally left blank.

APPENDIX A
APTOS SYSTEM REQUIREMENTS

ID	Level	Category	Requirement	Verification Method	Verification Plan
APT-REQ-1	0		The system shall improve the rocket's ability to maintain a vertical flight by minimising roll rate and pitch abd yaw Euler angles during ascent.	Analysis	Flight test
APT-REQ-1-1	1	Control System	The system shall be controllable in pitch, yaw and roll axes.	Analysis	Simulink models
APT-REQ-1-1-1	2	Control System	The system's performance and stability shall be robust to the expected variability in the construction of the rocket and module, with 95% accuracy and 95% confidence.	Analysis	Robustness analysis and Chernoff bound
APT-REQ-1-2	1	Control System	The system shall be observable in pitch, yaw and roll axes.	Analysis	Simulink models and sensor selection.
APT-REQ-1-3	1	Control Surfaces	The fins shall produce enough lift to overcome the rocket's corrective moment	Analysis	Aero load analysis.
APT-REQ-1-3-1	1	Control Surfaces	The fins shall be relatively easy to manufacture	Demonstration	Manufacture of Rocket
APT-REQ-1-3-2	1	Control Surfaces	The fins shall be easy to remove from rocket	Demonstration	On-ground test
APT-REQ-1-4	1	Control System	The system shall maintain Euler angles of the rocket within prescribed limits.	Analysis	Analysis of data collected during flight
APT-REQ-1-4-1	2	Control System	At launch velocity, the Euler angles should not exceed (in degrees): +-5 pitch, +-5 yaw, +-1 roll	Analysis	Analysis of data collected during flight
APT-REQ-1-4-2	2	Control System	At burnout velocity, the Euler angles should not exceed (in degrees): +-1 pitch, +-1 yaw, +-1 roll	Analysis	Analysis of data collected during flight
APT-REQ-1-5	1	Actuation	The actuation system shall be able to set the canard deflections to the correct positions.	Test	On-ground module test
APT-REQ-1-5-1	2	Actuation	The actuators shall respond to a 10deg step input with an accuracy of +-0.5deg and no overshoot outside these bounds.		On-ground module test
APT-REQ-1-5-2	2	Actuation	The actuators should have positional feedback	Inspection	Supplier data
APT-REQ-1-5-3	1	Actuation	The canards should be positioned in one horizontal plane	Inspection	Supplier data
APT-REQ-1-5-4	2	Actuation	The actuation system shall have a stall torque of at least 11 kgcm (assuming 15 degrees max angle of attack)	Inspection	Supplier data
APT-REQ-1-5-5	2	Actuation	The actuation system shall set the canard deflections with a minimum accuracy of 1 +- 0.1 degrees	Test	On-ground module test, check positions using measurements e.g. camera, rotary encoder
APT-REQ-1-5-6	2	Actuation	The actuators shall respond to a 10deg step input with a settling time of less than 0.1 seconds.		
APT-REQ-1-6	1	Control System	The system shall be able to determine the current orientation of the rocket.	Test	On-ground module test, flight test
APT-REQ-1-6-1	2	Control Software	The software shall be able to use sensor measurements to determine rocket orientation.	Test	On-ground module test, flight test
APT-REQ-1-6-2	2	Control Software	The software shall not be affected by sensor drift.	Test	On-ground module test, flight test
APT-REQ-1-7	1	Control System	The system shall be able to change it's operation based on it's velocity and altitude.	Test	On-ground module test, flight test
APT-REQ-1-7-1	2	Control Software	The software shall be able to use sensor measurements to determine rocket velocity and altitude.	Test	On-ground module test, flight test
APT-REQ-1-7-2	2	Electronics	The electronics hardware shall enable the velocity and altitude of the rocket to be determined.	Test	On-ground module test, flight test
APT-REQ-1-8	1	Mechanical Design	The module shall allow the controller to control the servos (drivetrain).	Test	On-ground module test, flight test
APT-REQ-1-8-1	2	Mechanical Design	The drivetrain should be rigid.	Test	Torsion tests (Apply force with hands)
APT-REQ-2	0		The system shall maintain structural integrity during flight.	Inspection	Does it break during flight?
APT-REQ-2-1	1	Control Surfaces	The active control surface shall not snap during flight.	Analysis	FEA Analysis
APT-REQ-2-2	1	Mechanical Design	The linkages shall remain intact during flight.	Test	Stress tests (Apply force with hands)
APT-REQ-2-3	1	Mechanical Design	The system casing shall not fracture during flight.	Test	Stress tests (Apply force with hands)
APT-REQ-2-4	1	Mechanical Design	The system shall not exert forces on the rocket that exceed the yield strength of the airframe.	Analysis	Hand calculations from aerodynamic load on fins.
APT-REQ-3	0	Mechanical Design	The system shall integrate with a rocket of 4" body diameter.	Inspection	Check dimensions in CAD
APT-REQ-3-1	1	Electronics/Mechanical Design	The electronics hardware shall fit within the constraints of the mechanical design of the module.	Inspection	Check fit in CAD
APT-REQ-3-1-1	2	Electronics/Mechanical Design	The module shall house the servo motors and fix them in place	Inspection	Check design in CAD

APT-REQ-3-1-2	2	Electronics/Mechanical Design	The module shall house the PCBs and batteries and fix them in place	Inspection	Check design in CAD
APT-REQ-3-1-3	2	Electronics/Mechanical Design	The module shall facilitate electrical connections that allow the controller to control the servos	Inspection	Check design in CAD
APT-REQ-3-2	1	Mechanical Design	The mass of the module shall not adversely stress the body tube	Inspection	Check design in CAD
APT-REQ-4	0		The system shall fail safely.		
APT-REQ-4-1	1	Control Software	The control system shall not crash in the case of hardware failure.	Test	Emulate hardware failure and verify software doesn't crash.
APT-REQ-4-2	1	Control System	The control system shall be robust to noise in sensor readings.	Analysis	Simulink robustness analysis.
APT-REQ-4-3	1	Control Software	The control surfaces shall deflect to zero in the event failure.	Test	Test each failure mode
APT-REQ-4-4	1	Control Software	The control surfaces shall align to zero when the orientation of the rocket is outside 20 degrees from vertical.	Test	Tilt module to 20 degrees
APT-REQ-4-5	1	System Integration	REMOVED	Test	Disconnect linkage and observe control surfaces
APT-REQ-4-6	1	Control Software	The control system shall record and save data, even in the case of an in-flight failure.	Test	Test black box (robustness)
APT-REQ-4-7	1	Electronics	The electronics shall have a robust power system.	Analysis	Design and calculations
APT-REQ-4-7-1	2	Electronics	The power system shall be easily charged between flights.	Analysis	Design and calculations
APT-REQ-4-7-2	2	Electronics	The power system shall be easily checked for voltage level before flight.	Analysis	Design and calculations
APT-REQ-4-7-3	2	Electronics	The electronics should handle all current and voltage loads.	Analysis	Design and calculations
APT-REQ-5	0	System Integration	The system shall be manufacturable in-house within time and budget constraints.	Demonstration	Compare to past rocket builds to estimate time and budget.
APT-REQ-5-1	1	System Integration	The materials should be environmentally sustainable.	Demonstration	Research materials before use.
APT-REQ-6	0		The rocket should fly higher with the Aptos module installed than without it.	Analysis	6DOF simulations with and without Aptos module installed.
APT-REQ-6-1	1	Electronics	The electronics hardware shall allow the control software to measure altitude during flight.	Inspection	Check electronics design
APT-REQ-7	0		The system shall be able to be controlled without disassembling the rocket.	Test	Module test
APT-REQ-7-1	1	Electronics	The electronics hardware shall allow communication with external devices without disassembling the rocket.	Test	Module test
APT-REQ-7-2	1	Control Software	The control software shall be controllable by external devices without disassembling the rocket.	Test	Module test
APT-REQ-7-3	1	Control Software	The control software shall be robust to connecting and disconnecting to external devices.	Test	Module test
APT-REQ-7-4	1	Control Software	The control software shall give feedback to external devices when changes are made or there are errors.	Test	Module test

APPENDIX B
XFLR5 GRAPHS

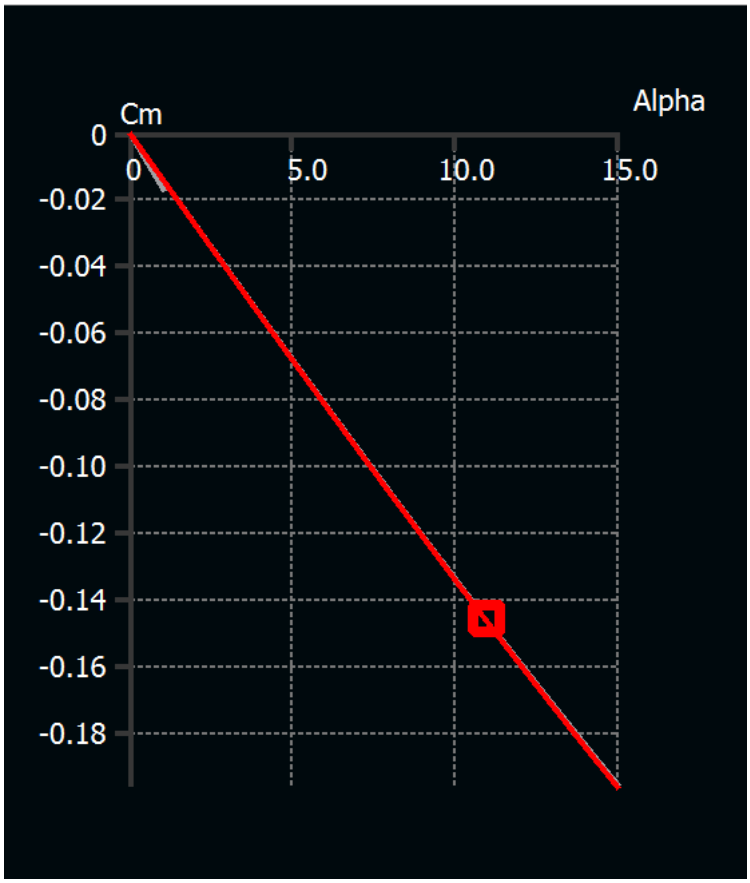

Fig 6. Canard Pitching Moment Coefficient vs Alpha from XFLR5

APPENDIX C
FLIGHT COMPUTER SYSTEM ARCHITECTURE

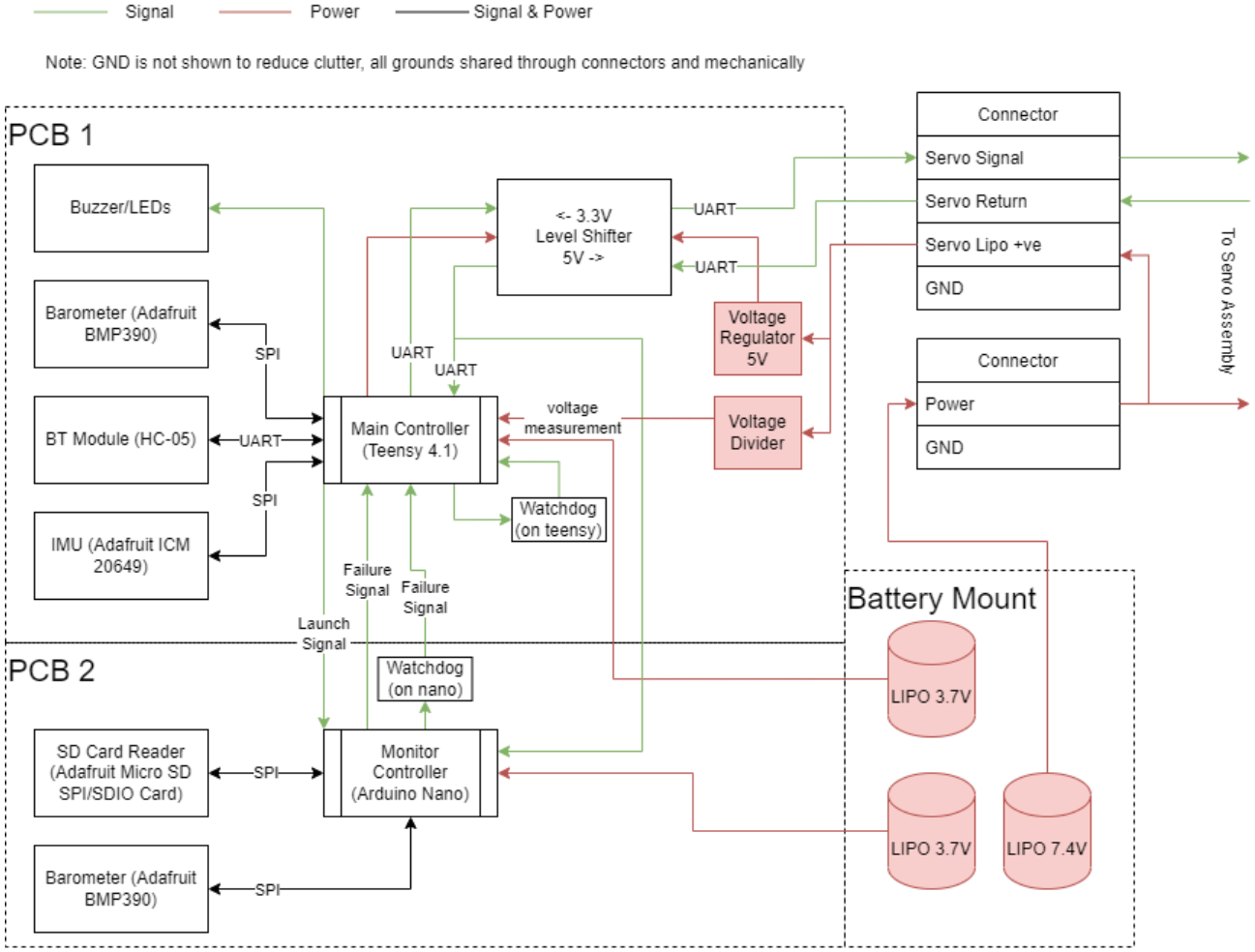

APPENDIX D
ELECTRONICS SCHEMATICS

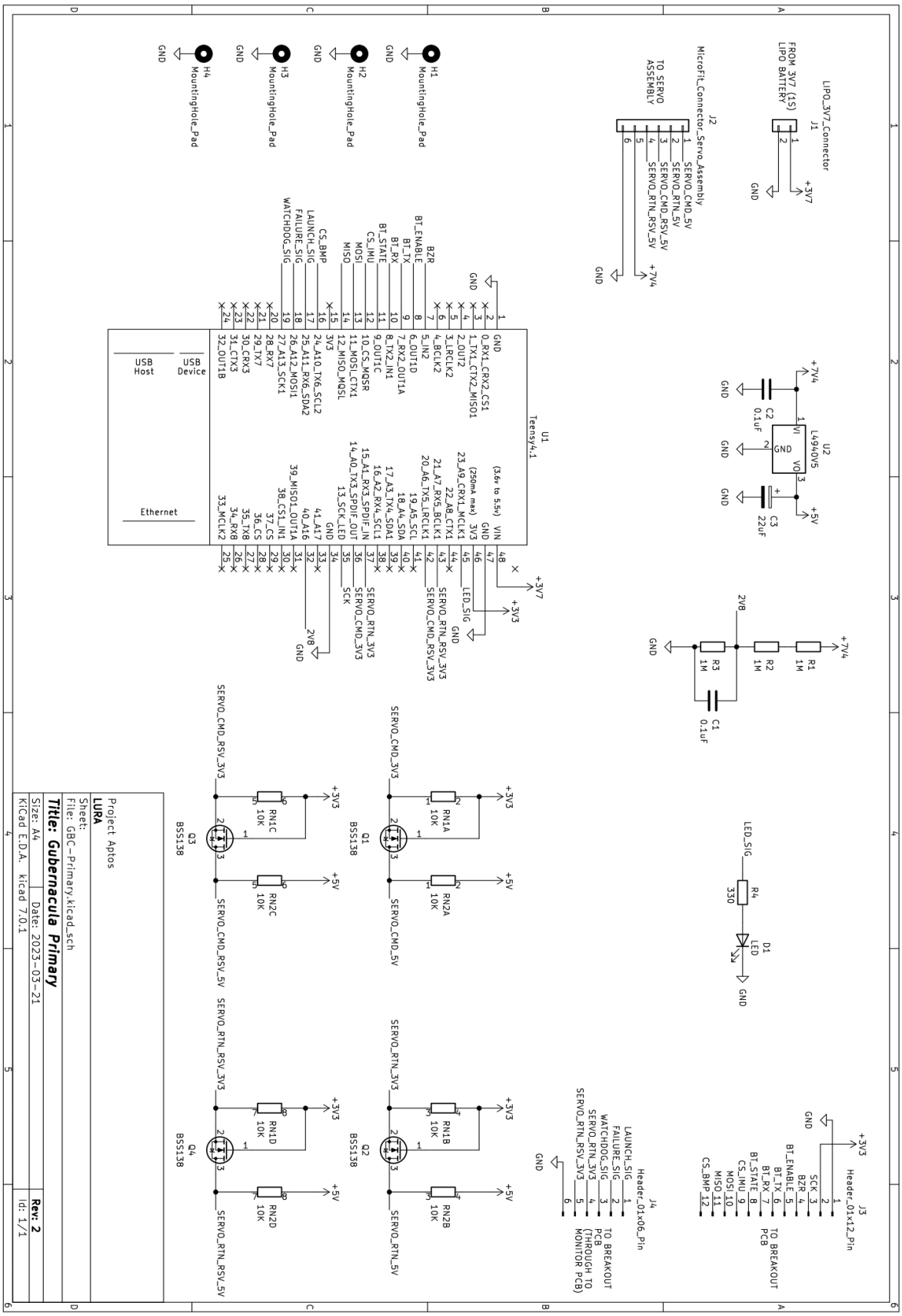

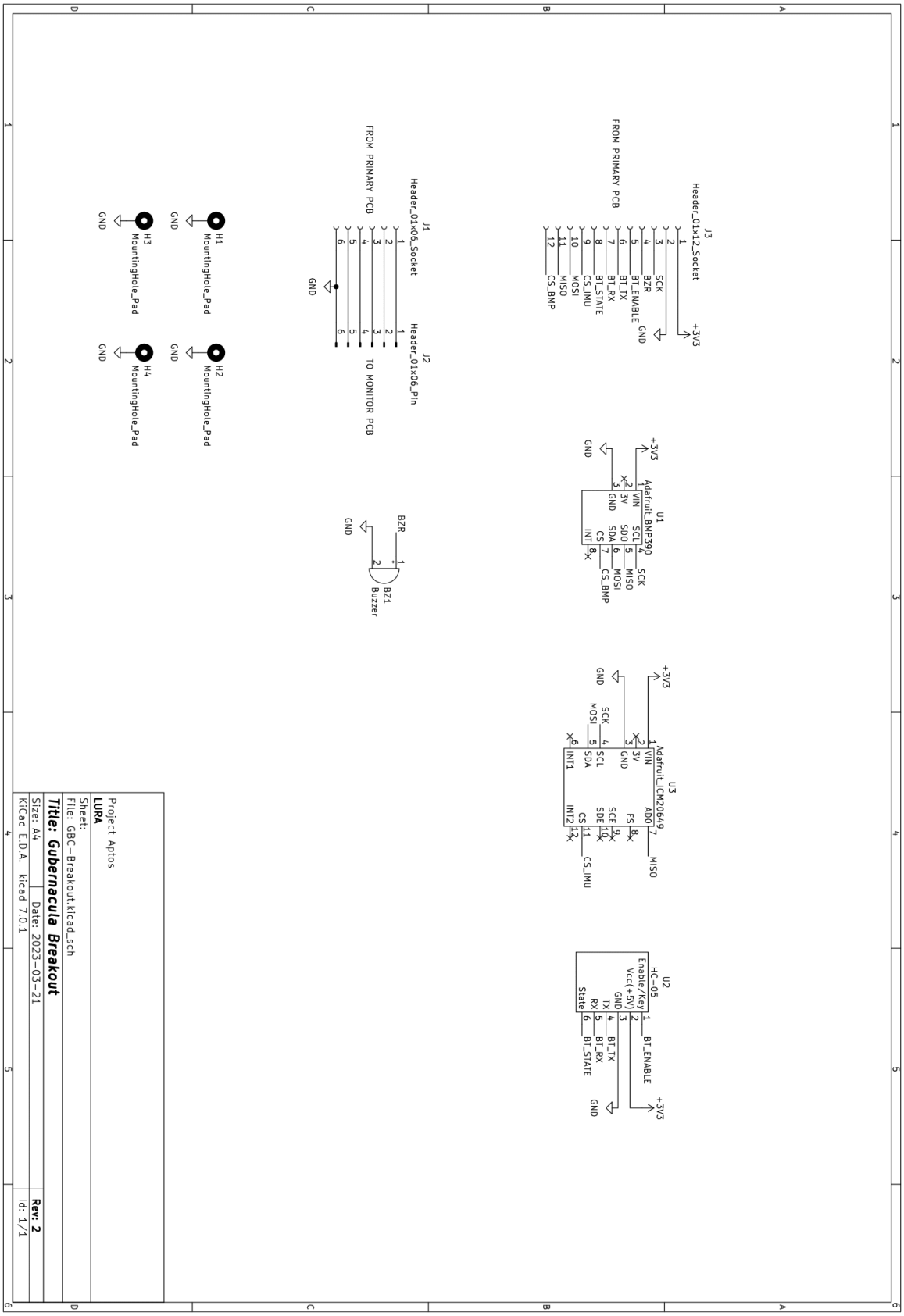
J3
Header_01x12_Socket
SCK
BZR
BT_ENABLE
BT_TX
BT_RX
BT_STATE
CS_JMU
MOSI
MISO
CS_BMP
+3V3
GND
FROM PRIMARY PCB
J1
Header_01x06_Socket
J2
Header_01x06_Pin
TO MONITOR PCB
BZR
BZ1
Buzzer
H1
MountingHole_Pad
H2
MountingHole_Pad
H3
MountingHole_Pad
H4
MountingHole_Pad
U1
Adafruit_BMP390
VIN
3V
SCL
SDO
SDA
CS
INT
U2
HC-05
Enable/Key
Vcc(+5V)
TX
RX
State
U3
Adafruit_ICM20649
ADO
FS
SCE
SDE
INT1
INT2
Project Aptos
LURA
Sheet:
File: GBC-Breakout.kicad_sch
Title: Gubernacula Breakout
Size: A4
Date: 2023-03-21
Rev: 2
KiCad E.D.A. kicad 7.0.1
Id: 1/1

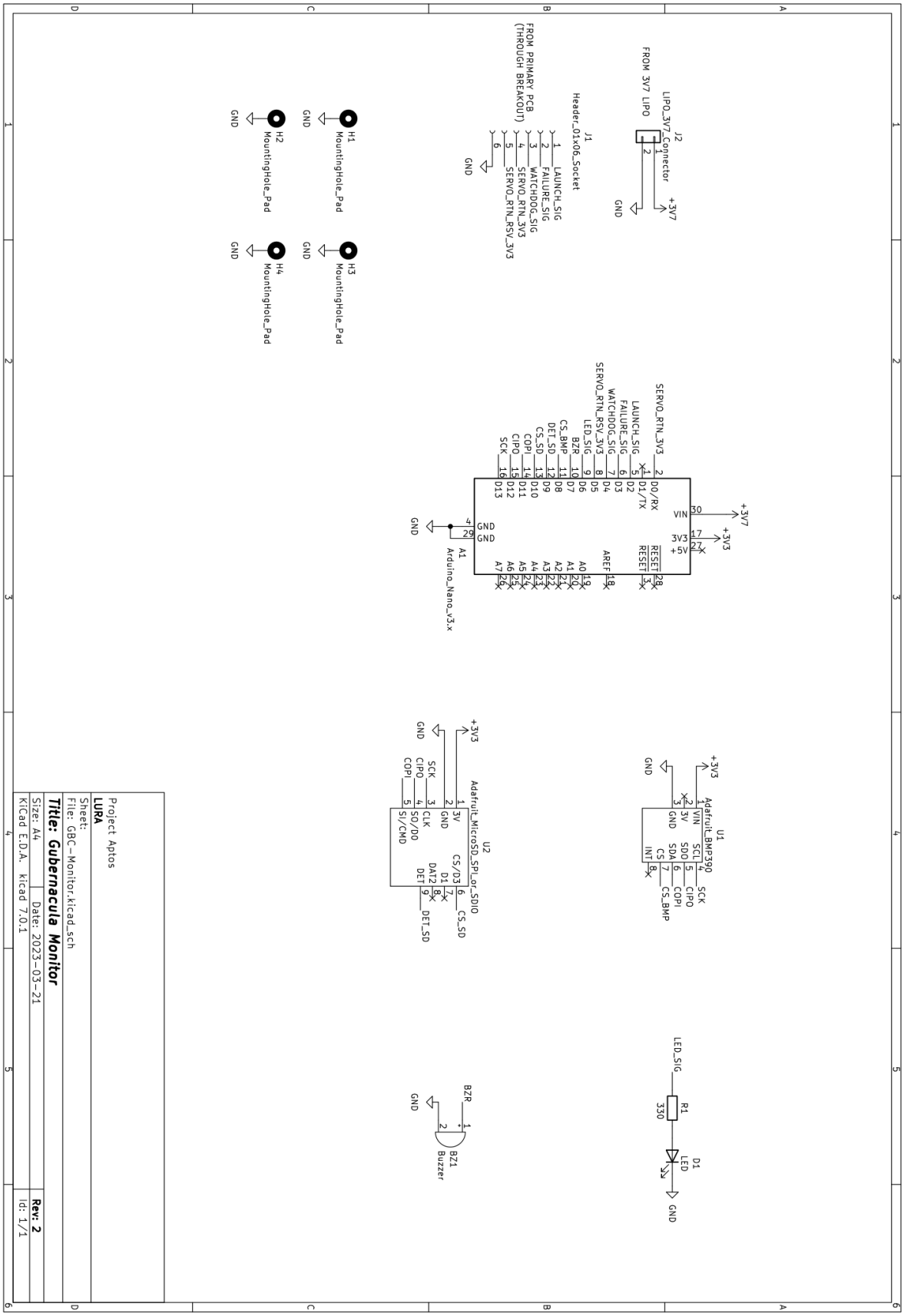
LIPO_3V7_Connector
FROM 3V7 LIPO
+3V7
GND
Header_01x06_Socket
FROM PRIMARY PCB (THROUGH BREAKOUT)
LAUNCH_SIG
FAILURE_SIG
WATCHDOG_SIG
SERVO_RTN_3V3
SERVO_RTN_RSV_3V3
Arduino_Nano_v3.x
MountingHole_Pad
Adafruit_BMP390
Adafruit_MicroSD_SPI_or_SDIO
LED
Buzzer
R1
330
Project Aptos
LURA
Sheet:
File: GBC-Monitor.kicad_sch
Title: Gubernacula Monitor
Size: A4
Date: 2023-03-21
KiCad E.D.A. kicad 7.0.1
Rev: 2
Id: 1/1

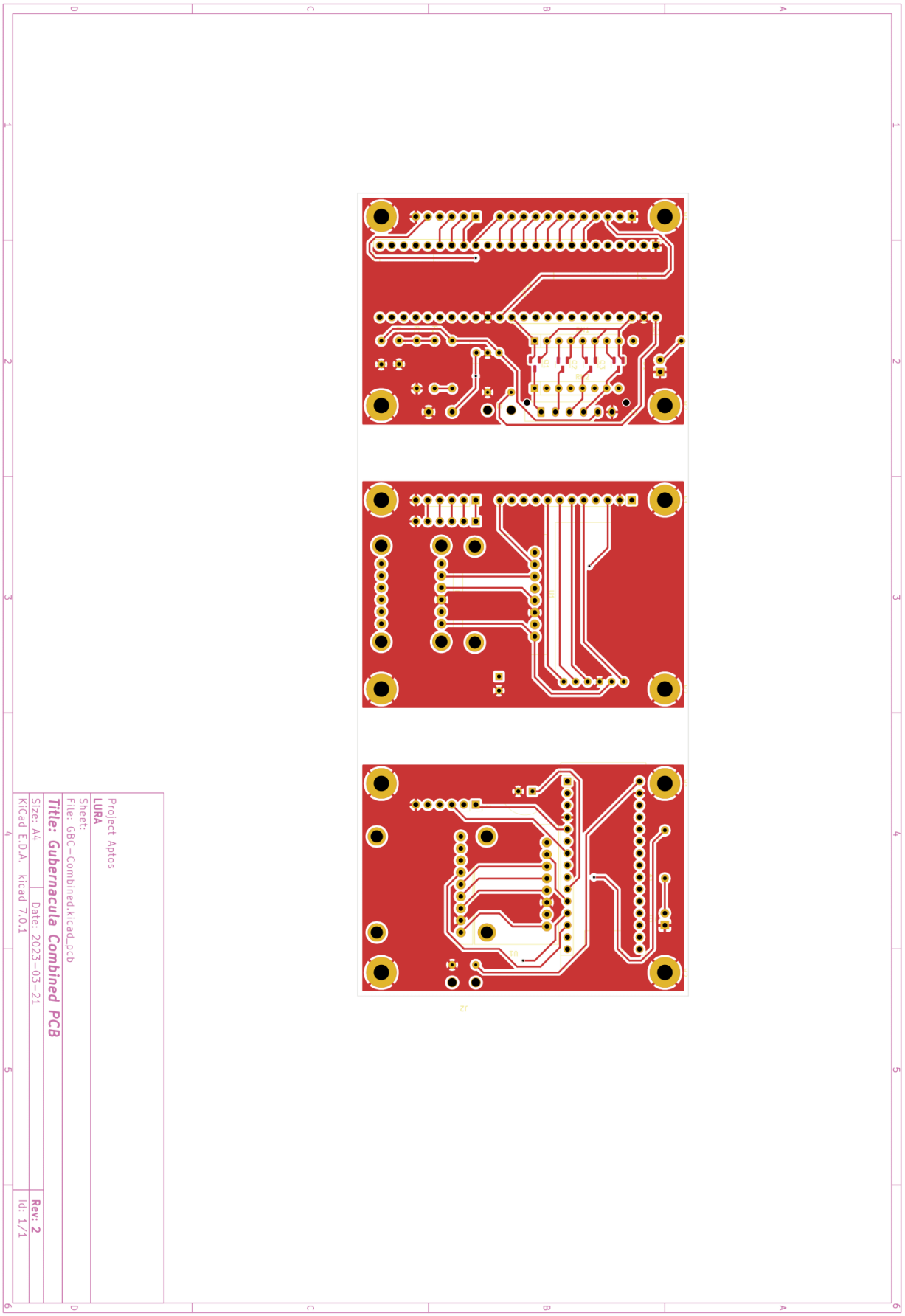
Project Aptos
LURA
Sheet:
File: GBC-Combined.kicad_pcb
Title: Gubernacula Combined PCB
Size: A4
Date: 2023-03-21
KiCad E.D.A. kicad 7.0.1
Rev: 2
Id: 1/1

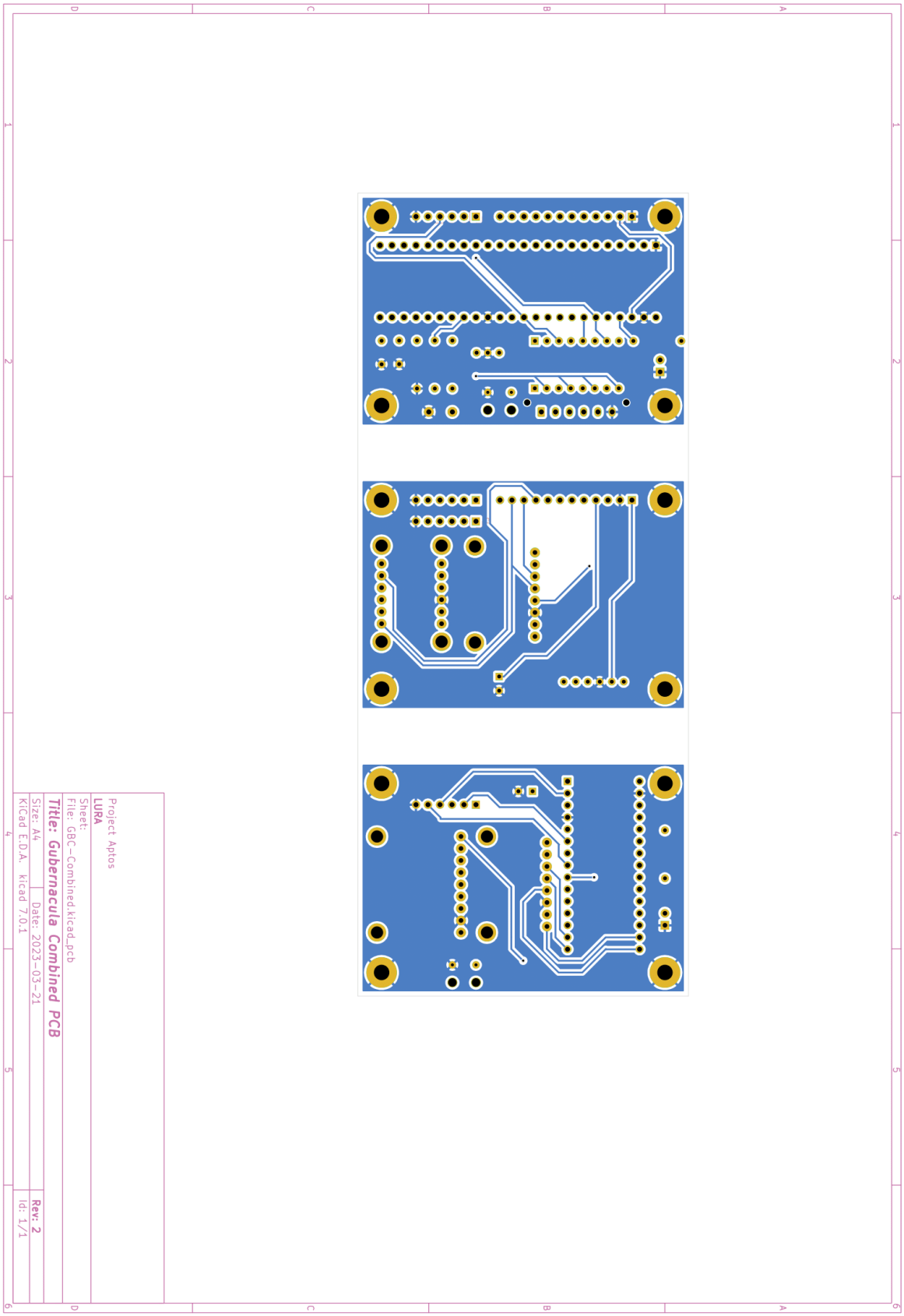
Project Aptos
LURA
Sheet:
File: GBC-Combined.kicad_pcb
Title: Gubernacula Combined PCB
Size: A4
Date: 2023-03-21
KiCad E.D.A. kicad 7.0.1
Rev: 2
Id: 1/1

APPENDIX E
TECHNICAL DRAWING PACK